RD51, a world-wide collaboration for the development of Micro Pattern Gaseous Detectors

M. Chefdeville

RD51, a world-wide collaboration for the development of Micro Pattern Gaseous Detectors

M. Chefdeville, on behalf of the RD51 collaboration
Laboratoire d'Annecy-le-Vieux de Physique des Particules, 9 Chemin de Bellevue - BP 110, 74941 Annecy-le-Vieux CEDEX - FRANCE

E-mail: chefdevi@lapp.in2p3.fr

Abstract. Originally introduced to improve the rate capability of traditional wire chambers, Micro Pattern Gaseous Detectors (MPGD) actually demonstrate many more benefits. Be it for medical and industry imaging, collider experiments or more interestingly in the framework of this conference for the search of rare events, they are the subject of constant research and development in several laboratories over the world. The RD51 collaboration has been coordinating this work since April 2008 and is meant to advance the technological development and application of MPGD. The collaboration is presented and emphasis is put on its latest achievements which do make these devices an attractive option for the detection of low energy rare events: the possibility to instrument large area and to detect UV photons.

1. Introduction

1.1. Micro Pattern Gaseous Detectors

An experimental fact familiar to gaseous detector physicists is the drop of gas gain of wire chambers above some rate. This limit rate primarily depends on the collection time of the avalanche ions, the space charge of which reduces the applied field. As a result of the rapidly decreasing radial field around the wire, the intrinsically low mobility of ions and the relatively large wire to cathode distance (1–10 mm), the maximum sustainable rate hardly exceeds 10 kHz/mm^2. With thin alternating cathode and anode strips printed on a substrate at a few hundred micron pitch, the Micro Strip Gas Counter [2] is considered as the first Micro Pattern Gaseous Detector. In spite of a poor robustness against discharges its invention in 1988 is a major breakthrough in the field of gaseous detectors, paving the way for higher rate operation. The fast collection of ions in MSGC indeed pushes the rate capability by two order of magnitude with respect to wire chambers, up to roughly 1 MHz/mm^2 [3].

Stimulated by the progress in printed circuit board (PCB) technology, the invention of the Micro Mesh Gaseous Structure (Micromegas [4]) and the Gas Electron Multiplier (GEM [5]) followed in 1996 and 1997 respectively. Compared to MSGCs, they show even higher rate capability [6]. Their functioning is easily grasped in Figure 1 where drawings of the electrodes and electric field lines are shown. Based on Micromegas and GEM geometry, other detectors with specific advantages have been developed. Non exhaustively, they are the micro-Bulk, Thick GEM (THGEM [7]), Resistive Electrode Thick GEM (RETGEM [8]), Resistive mesh detectors [9], Micro Hole Strip Plate (MHSP [10]) and the GridPix [11]. Stacking GEMs or combining different technologies is possible, for instance to increase the total gain [12, 13] or reduce ion feedback to the drift space or top electrodes [14].

Optimised MPGD show great performance: gas gains close to the breakdown limit (10^6–10^7 for single electrons), spatial resolution of a few tens of microns [15, 16], timing capability with MIPs of a few ns [18] and below the ns as photodetector [17], energy resolution close to the statistical limit (11.7 % and 1 % FWHM to 5.9 keV X-rays and 5.5 MeV alphas respectively [19, 20]), ion backflow fractions (IBF) of a few 10^{-3} [14, 21]. Finally, MPGD can be made sensitive to photons in the UV range with coatings of the electrodes with photoconverting materials like CsI [17, 22].

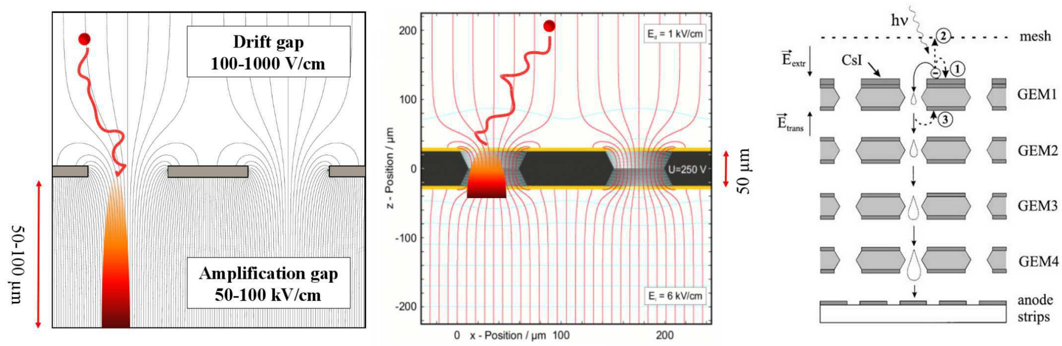

Figure 1. Illustration of the working principle of Micromegas (left), single (center) and cascaded (right) GEM. The electron multiplication occurs in the high field region between the mesh and the anode plane in the case of Micromegas and inside the GEM holes.

1.2. The RD51 collaboration

The RD51 collaboration goal is to advance the technological development and application of MPGD [23]. It coordinates the efforts of several universities and research laboratories from 25 countries in Europe, America, Asia and Africa. It is organised in working groups, each with objectives, tasks and regular meetings for sharing information, results and experience. The collaboration tries to optimize the cost of R&D projects by sharing resources, creating common projects and providing common infrastructures. The main objectives of the collaboration can be summarized as follows:

- the development of fabrication techniques and production facility of large area detectors which also includes industrial partnership to increase mass production capability;
- the understanding of the physical phenomena limiting the performance of current MPGD and the definition of test standards for comparison between different detector technology;
- the development of common software, test infrastructure and readout systems.

For a more detailed description of the working groups the reader is referred to [24].

1.3. Detection of rare events with MPGDs

Micro Pattern Gaseous Detectors can be applied as the readout of calorimetric or tracking devices for the search of rare events like neutrino scattering off nuclei, dark matter interactions and neutrino-less double-beta decays. On-going projects using gas/liquid media as well as some proposals for future experiments are based on large Time Projection Chambers (TPCs) filled with liquefied noble gases (see [25, 26] for reviews of experiments, projects and proposals). Argon and xenon are targets of choice for the detection of dark matter because of their high density. They do moreover scintillate with a high photon yield allowing the discrimination of backgrounds by measuring the ionisation density through the ratio of scintillation light to charge.

This dark detector has to be sensitive to UV light and to provide good light resolution over large area. Charge resolution may also be required if the primary ionisation is to be directly detected rather than converted into light through scintillation in moderate electric fields. Another TPC application is the search for the neutrino-less double-beta decay of ^{136}Xe. Here, the TPC is used to precisely measure the energy of the two emitted electrons and equipped so as to trap and identify the daughter ^{136}Ba ion by laser spectroscopy. Clearly, excellent energy resolution is mandatory to distinguish the neutrino-less decay peak in the tail of the standard double beta decay energy spectrum.

The capability to cover large area with uniform response and an excellent energy resolution are essential ingredients which are partly determined by the fabrication techniques of MPGD. These techniques are detailed in the next section with examples of running experiments or current projects within the RD51 collaboration. Also related to large area detectors is the development of a readout system that can be applied to different MPGD and easily scales with the number of channels. This RD51 development is motivated in section 3 where its recent successful implementation with a detector is presented. Finally, the detection of UV light with MPGD-based photomultipliers relevant to the detection of rare events is discussed.

2. Fabrication of large area detectors

2.1. Micromegas

First Micromegas were made of a few micron thin electroformed nickel mesh subsequently stretched and glued on an insulating frame which is then placed on a flat PCB dressed with photolithographically printed pillars and readout electrodes. Possible wrinkles of the mesh would disappear upon application of some voltage difference between the mesh and the anode as the electric force pulls the mesh toward the PCB. This assembly process is not straightforward and a simpler procedure called Bulk has been proposed [27].

The Bulk Micromegas consists of a woven wire mesh. Available in rolls of 24×40 m^2, the mesh is solidly mounted on the PCB in a single process. The anode plane, a photoresistive film, the mesh and a second film are laminated at high temperature. The pillars are then formed by photolithography. Facts and figures about standard Bulk are: stainless steel 30 μm diameter wires woven at a pitch of 80 μm, an anode to mesh distance of 128 μm, a pillar diameter and pitch of 300 μm and 2 mm respectively and similar gas gain property as electroformed Micromegas.

The principal production facility is the CERN workshop where detector sizes up to 150×50 cm^2 are currently obtained. The CERN management is supporting future upgrade of some LHC sub-detectors with large area MPGD. Accordingly it has approved the construction of a new workshop and its equipment with new machines of larger size processing capability. Eventually, the fabrication of Bulk Micromegas with active areas up to 2×1 m^2 will be possible.

2.2. Large-area Micromegas experiments and projects

Bulk Micromegas has been chosen by the T2K collaboration to equip the 3 TPC of the off beam axis detector [28]. Each TPC has a central cathode plane of 2×0.7 m^2 and two end-plates of 12 modules (fig. 2 left). Individual modules are equipped with 1726 readout channels and have a size of 34×36 cm^2, 95 % of which is active. The distance between adjacent modules is such that 85 % of the end-plate is active. Pad by pad X-ray characterisation of the modules in a dedicated test chamber revealed a uniformity of the photopeak position of 3 % and an RMS dispersion of the mean peak position of all 72 modules of about 8 %. Since January 2010, the three TPCs are operational and successfully took data during the first T2K physics run.

A modular approach to the construction of large area Bulk chambers is also adopted by a group of the Calorimeter for linear collider experiment collaboration (CALICE) [29]. The mid-term goal of the project is the construction of a 1 m^3 sampling hadronic calorimeter with thin Micromegas chambers as active media interleaved with steel absorbers. Six modules of 48x32 cm^2

with square pad of 1 cm^2 are assembled in a same gas volume. With 1 mm between each module and 2 mm wide inactive borders, dead regions amount to less than 3 % of the chamber area. A first prototype was constructed and tested in beam in 2010. A technical challenge here is the embedding of the front-end electronics on the Bulk PCB inside the chamber while keeping the total thickness below 12 mm.

An example of large area coverage with a single Bulk mesh is the ATLAS muon chamber upgrade project undertaken by the MAMMA collaboration [30]. The increase of luminosity and thus of rate foreseen at super LHC will impose the replacement of the Cathode Strip Chambers (CSC) in the forward ATLAS muon system. Micromegas chambers, thanks to their high rate capability have been chosen for this upgrade and first prototypes of the size of half a CSC have been constructed (wedge-shaped and of roughly 100×50 cm^2, fig. 2 center). When voltage is applied to the mesh, a large energy can be released in the front-end electronics upon discharges. That makes spark protections essential for the stable operation of such large area single mesh detectors. Within the RD51 collaboration, protections using resistive strips have been successfully tested on small prototypes and are now applied on full scale chambers.

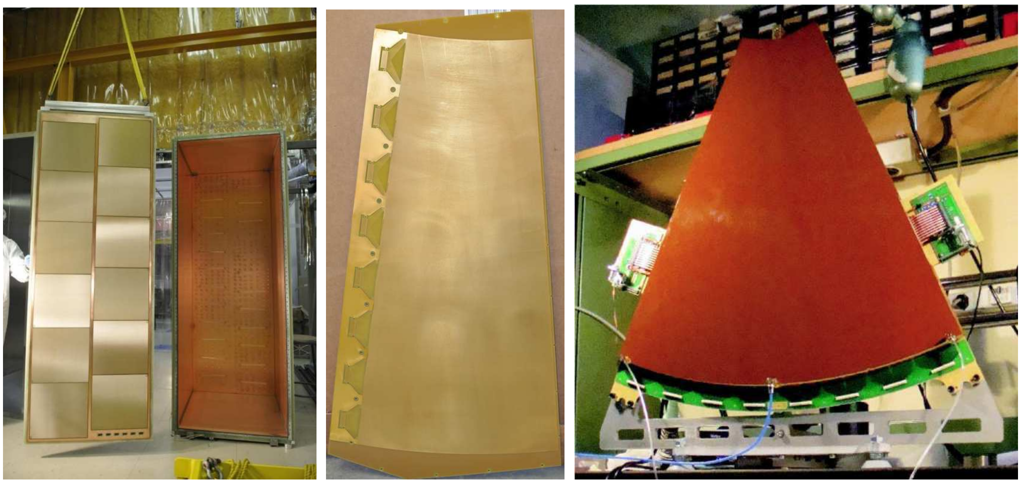

Figure 2. From left to right: photograph of a TPC for T2K showing an endplate (0.7×2 m^2) with Micromegas modules and the field cage; 1 m long Bulk mesh with strip readout for Super ATLAS; triple GEM chamber for the TOTEM tracking system (0.2 m^2).

2.3. GEM
Standard GEM foils are fabricated using a double-mask photolithography process. The raw material is usually 50 μm thick kapton with a 5 μm copper cladding on both sides. The hole pattern (50–100 μm diameter at 100–200 μm pitch) is transferred from flexible masks to the top and bottom copper surfaces by photolithography and the kapton is removed by wet etching. The alignment between the top and bottom masks is crucial to insure a good uniformity of the hole geometry across the GEM surface. It becomes however awkward for area larger than 40×40 cm^2. Moreover, the width of the raw material is limited to roughly 60 cm which is another obstacle to fabricate larger area GEMs. These two limitations have recently been overcome with the introduction of a single-mask process and a new technique to splice foils with minimum dead zone at the junction. The key of the process is to use the top copper layer (patterned by photolithography) as a mask to remove the kapton; the patterned kapton then acts as a mask to etch the bottom copper layer [31]. At the moment of writing, the size of single GEM foils produced at the CERN workshop is 70×40 cm^2, limited by the machine dimensions. After the

upgrade of the workshop (mentioned in the previous section), the fabrication of GEM foils of 200×50 cm^2 will be possible.

2.4. Large area GEM projects

Single-mask GEMs are foreseen for the upgrade of the tracking stations of the TOTEM experiment at LHC [32]. A prototype based on 66×66 cm^2 foils spliced together demonstrated the possibility to instrument large area, in that case 0.2 m^2 (fig. 2 right). It consists of a stack of three GEMs, each electrode being connected to a voltage divider chain. Triple GEMs are also considered to extend the forward region of the CMS muon spectrometer in the rapidity region above 1.6 [33]. In 2010, a first prototype was fabricated and tested in a high energy particle beam. Of trapezoidal shape, it is 1 m long with a total area of about one third of a m^2. In order to avoid possible damage of the GEM foils by discharges, they are segmented in several sectors so as to reduce the electric energy stored in the foils.

The relative fragility of GEM against discharges can be overcome by segmentation of the foils. It also motivated the development of the so-called Thick-GEM [7] which is a GEM with dimensions (thickness, hole diameter and pitch) scaled up by a factor of ten roughly. Based on relatively cheap and simple production techniques they are robust and suitable for the fabrication of large detectors. Single THGEMs do show high gas gains (10^5) and even higher when stacked (10^7) [34]. They are an alternative to GEM for applications where the requirements on spatial resolution are not too stringent (sub-mm).

3. A multi-channel scalable readout system of MPGD

3.1. Concept of the Scalable Readout System

In parallel to the fabrication of large area MPGD, an important mission of the RD51 collaboration is the development of a portable multi-channel readout system of scalable architecture. This so-called Scalable Readout System (SRS) can be applied to small test systems as well as large LHC like systems and should insure protection of the front-end electronics against discharges. It is also intended for facilitating the access of RD51 groups to electronics and for avoiding parallel developments of very similar systems.

The SRS architecture is composed of a detector specific part (the ASIC), a front-end concentrator card (FEC) which can also perform signal digitization, a Scalable Readout Unit (SRU) for multiplexing data when more than one FEC is used and a PC with DAQ and slow-control software and analysis framework (fig. 3 left). The SRU multiplexes data from up to 36 FEC which is about several tens of thousand channels. Even larger systems can be implemented with multiple SRS.

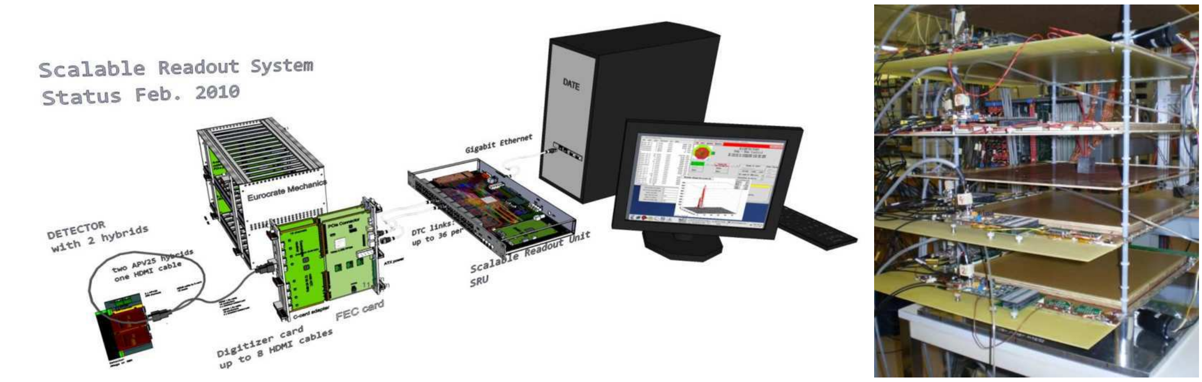

Figure 3. Sketch of a complete Scalable Readout System from front-end chip to computer (left). Photograph of a minimal muon tomography station consisting of GEM chambers of 30×30 cm^2.

3.2. First implementation of the SRS in a GEM detector
The first complete small SRS has become available in fall 2010 and was successfully applied to the readout of GEM tracking stations for muon tomography [35]. The project aims at detecting and imaging heavily shielded high-Z nuclear materials such as enriched uranium by exploiting multiple scattering of cosmic muons [36]. A minimal tomography station based on several Triple GEM chambers of 30×30 cm^2 equipped with two sets of 768 strips running in both X and Y directions was realised. Tests performed over a small active area with preliminary electronics demonstrated the capability to image medium and high-Z targets of small volumes [37].

In a second step, entire Triple GEM chambers (1536 channels/chamber, fig. 3 right) were read out, one by one, with a small SRS. The system consists of 12 front-end hybrid boards based on an analogue amplifier chip, which are connected via HDMI cables to a pair of ADC/FEC electronics cards. A Gb-ethernet link connects the small-system SRS electronics to a Linux PC running DATE on-line data acquisition software developed for the ALICE experiment. The ROOT-based ALICE/AMORE package is used for on-line and off-line data analysis. The full chain from GEM detector to off-line analysis was made operational within one day and enabled to take data continuously during several days. The group is now working on the production of the full SRS electronics so as to equip 10 tracking stations (≈16 thousand channels). This first successful implementation of the SRS is very promising and should benefit to other large area MPGD projects in the future.

4. Photomultipliers based on MPGDs
4.1. Introduction
Gaseous detectors have some unique advantages over vacuum-based and solid-state devices (PMT, MCP and SiPM) for the detection of single UV photons. They can operate in a magnetic field and as far as large area coverage is concerned, they are the most cost effective solution and involve little material budget (see [38] and references therein). Three generations of gaseous PM can be distinguished: the first is based on the addition of a photoconverting vapour (TMAE, TEA) to the detector atmosphere where photons enter through a transparent window. The second generation consists of a wire chamber with CsI coated cathode pads. The most popular photocathode material is CsI. Because of a relatively high work function it is more robust than others used in vacuum-based detectors. The production of CsI photocathodes has been optimised and presently quantum efficiency of 27 % at 170 nm are routinely obtained. Maintaining the efficiency to its original value, however, is difficult above a collected charge of some mC/mm^2. This ageing phenomenon is caused by the impact of avalanche ions and photons onto the cathode surface and prevents operation at high gas gain and/or rate. The new generation of gaseous PMs combine MPGD with photosensitive coatings to reduce feedback mechanisms and improve the rate capability. Their functioning is illustrated with two leading projects of the RD51 collaboration: the development of Ring Imaging Cerenkov and cryogenic detectors.

4.2. Ring imaging Cerenkov detectors
A typical arrangement of GEM-based photomultiplier taken from [14] is showed in Figure 1 (right). CsI is evaporated on the top metal layer of the first foil. With optimised field settings and gas composition photoelectrons are efficiently transferred to the first GEM holes where they are multiplied. Multi-staged structures have the advantage that the photocathode is fully concealed from avalanche photons. Distribution of the gain over the various GEMs allows very large total gains of 10^6–10^7 to be achieved [34]. Moreover, most of the ions are produced at the bottom GEM and have a high probability to be captured on some electrodes before reaching the photocathode. The exact ion backflow fraction is a complex function of the fields and foil geometry. Typical values are of the order of some 10^{-3} at a total gain of 10^4 and decrease further at higher gains.

Photosensitive GEM stacks can operate in pure CF_4 as a window-less Cerenkov detector; the gas acting both as a radiator and a charge amplification medium. A conductive mesh placed above the stack and set at the same voltage as that of the top electrode collects the primary charge from charged particles traversing the gas. As a result, only particles emitting Cerenkov radiation in the gas atmosphere are detected. These so-called Hadron Blind Detectors (HBD) find application for instance in the PHENIX experiment at RHIC where they are used at identify low momentum electrons in a high density hadron environment [39].

Cascaded GEM with CsI coatings are also considered for extending the particle identification capability of the ALICE RICH to higher momenta. Several optimisation studies are being carried out in view of this application [40]. For instance: the use of THGEM to achieve very high gas gain, the introduction of new foil geometry with ion-trapping electrodes ([10, 41]) to reduce the IBF below 10^{-3} and the measurement of photoelectron extraction efficiency versus electric field in various gas mixtures to maximize the single photon sensitivity.

4.3. Cryogenic application in double phase TPC

Liquefied noble gas filled TPCs have been proposed for the direct detection of dark matter. This technique makes use of both charge and scintillation signals produced by interacting particles in the liquid (fig. 4 left). CsI-coated multi-stage MPGD could be applied as the readout of double-phase TPCs with or without separation of the two phases by a window. In both cases, cryogenic temperatures result in high molecular density which can possibly lower the photoelectron extraction efficiency. Moreover, the window-less design implies that the amplifying structures are standing in a quencher-free atmosphere of a high-purity noble gas where high gains are difficult to achieve. The operation of MPGD at low temperature is thus a real challenge undertaken by several groups who study the performance of GEM-based prototypes in various noble gases at low temperature or high pressure [42, 43]. A successful example of this research is the detection, a few years ago, of both primary scintillation and ionisation signals produced by β-electrons in liquid argon in a triple GEM chamber [44]. The experimental set-up and scintillation and charge signals are shown in fig. 4 center and right respectively.

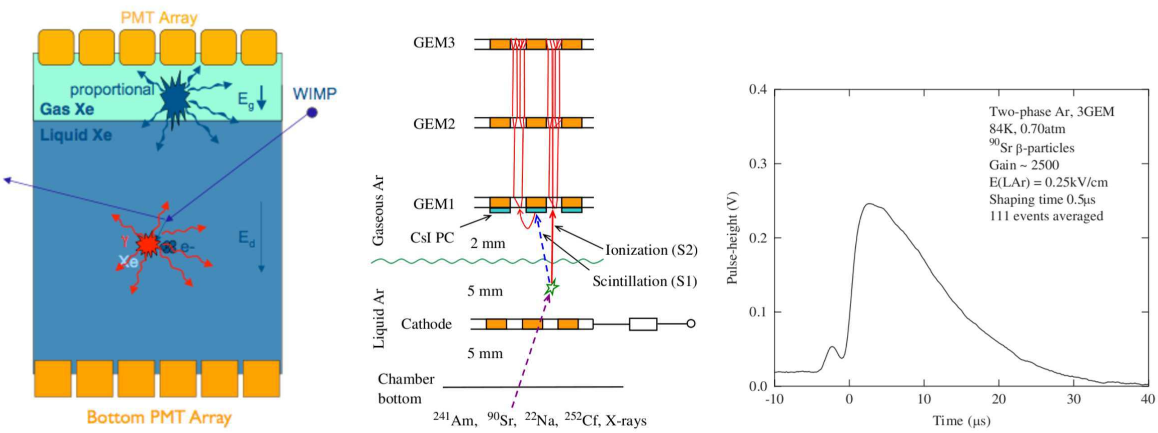

Figure 4. From left to right: concept of the detection of WIMP with double phase TPC; schematic view of an experimental set-up to study the performance of a small two-phase argon detector with CsI coating; top GEM signals (averaged over 111 events) induced by ^{90}Sr β-electrons, the scintillation signal is the small peak, prior to the higher ionisation signal. The center and right pictures are taken from [44].

5. Conclusion

Some fifteen years after their invention, Micro Pattern Gaseous Detectors have become inescapable in the landscape of particle detection. Precise, fast and versatile, they are the subject of constant research to understand their basic functioning and to reinforce and extend their application in various fields of science and industry. The RD51 collaboration is coordinating world-wide efforts in this direction such as the development of large area detector fabrication techniques and of a common multi-channel scalable readout system. Besides this, the capability of MPGD to detect UV photons is a topic of constant interest. It has been underlined in these proceedings as it paves the way for the search of rare events with MPGDs.

References

[1] A. Oed *Nucl. Instr. Meth. and Meth.* A **471** (2001) 109.
[2] A. Oed *Nucl. Instr. Meth. and Meth.* A **263** (1988) 351.
[3] F. Sauli, A. Sharma, *Annu. Rev. Nucl. Part. Sci.* **49** (1999) 341.
[4] Y. Giomataris et al. *Nucl. Instr. Meth. and Meth.* A **376** (1996) 29.
[5] F. Sauli *Nucl. Instr. Meth. and Meth.* A **386** (1997) 531.
[6] G. Charpak et al. *Nucl. Instr. Meth. and Meth.* A **412** (1998) 47.
[7] R. Chechick et al. *Nucl. Instr. Meth. and Meth.* A **535** (2004) 303.
[8] G. Agòcs et al. *JINST* **3** (2008) 02012.
[9] V. Peskov et al. *Nucl. Instr. Meth. and Meth.* A *In Press.*
[10] A. Breskin et al. *Nucl. Instr. Meth. and Meth.* A **553** (2005) 46.
[11] H. van der Graaf *Nucl. Instr. Meth. and Meth.* A **580** (2007) 1023.
[12] S. Bachmann et al. *Nucl. Instr. Meth. and Meth.* A **471** (2001) 115.
[13] P. Fonte, V. Peskov and B.D. Ramsey *Nucl. Instr. Meth. and Meth.* A **419** (1998) 405.
[14] A. Bondar et al. *Nucl. Instr. Meth. and Meth.* A **496** (2003) 325.
[15] J. Derré and I. Giomataris *Nucl. Instr. Meth. and Meth.* A **477** (2002) 23.
[16] B. Ketzer et al. *Nucl. Instr. Meth. and Meth.* A **535** (2004) 314.
[17] J. Derré et al. *Nucl. Instr. Meth. and Meth.* A **449** (2000) 314.
[18] G. Bencivenni et al. *Nucl. Instr. Meth. and Meth.* A **478** (2002) 245.
[19] A. Delbart et al. *Nucl. Instr. Meth. and Meth.* A **461** (2001) 84.
[20] T. Dafni et al. *Nucl. Instr. Meth. and Meth.* A **608** (2009) 259.
[21] I. Giomataris, P. Colas and V. Lepeltier *Nucl. Instr. Meth. and Meth.* A **535** (2004) 226.
[22] D. Mörmann et al. *Nucl. Instr. Meth. and Meth.* A **478** (2002) 230.
[23] Collaboration webpage: http://rd51-public.web.cern.ch/RD51-Public/
[24] S. Duarte Pinto, *Proc. of the XLVII Int. Winter Meeting on Nucl. Phys.*, Bormio (2009) 26.
[25] D. Akimov *Nucl. Instr. Meth. and Meth.* A **628** (2011) 50.
[26] F.T. Avignone, S.R. Elliott and J. Engel *Rev. Mod. Phys.* A **80** (2008) 481.
[27] I. Giomataris et al. *Nucl. Instr. Meth. and Meth.* A **560** (2006) 405.
[28] A. Delbart *Nucl. Instr. Meth. and Meth.* A **623** (2010) 105.
[29] C. Adloff et al. *JINST* A **4** (2009) 11023.
[30] T. Alexopoulos et al. *Nucl. Instr. Meth. and Meth.* A **617** (2010) 161.
[31] M. Villa et al. *Nucl. Instr. Meth. and Meth.* A **628** (2011) 182.
[32] G. Anelli et al. *JINST* A **3** (2008) 08007.
[33] D. Abbaneo et al. RD51 internal note RD51-Note-2010-005.
[34] A. Breskin et al. *Nucl. Instr. Meth. and Meth.* A **623** (2010) 132.
[35] L.J. Schultz et al. *Nucl. Instr. Meth. and Meth.* A **519** (2004) 687.
[36] K. Gnanvo et al. RD51 internal note RD51-Note-2010-004.
[37] K. Gnanvo et al., Submitted for publication in *Nucl. Instr. Meth. and Meth.* A, arXiv:1007:0256.
[38] S. Dalla Torre *Nucl. Instr. Meth. and Meth.* A *In Press*
[39] A. Kozlov et al. *Nucl. Instr. Meth. and Meth.* A **523** (2004) 345.
[40] M. Alexeev et al. *Nucl. Instr. Meth. and Meth.* A **623** (2010) 129.
[41] J.F.C.A. Veloso et al. *Nucl. Instr. Meth. and Meth.* A **581** (2007) 261.
[42] A. Bondar et al. *Nucl. Instr. Meth. and Meth.* A **556** (2006) 273.
[43] A. Breskin et al. *Nucl. Instr. Meth. and Meth.* A *In Press*
[44] A. Bondar et al. *Nucl. Instr. Meth. and Meth.* A **598** (2009) 121.